A Computationally Efficient Algorithm to Find Time-Optimal Trajectory of Redundantly Actuated Robots Moving on a Specified Path

Saeed Mansouri[1], Mohammad Jafar Sadigh[2], and Masoud Fazeli[3]
[1]Department of Mechanical Engineering, Sharif University of Technology, Tehran, Iran
[2]School of Mechanical Engineering, College of Engineering, University of Tehran, Tehran, Iran
[3]Department of Mechanical Engineering, Isfahan University of Technology, Isfahan, Iran

arXiv:1703.00151v1 [math.OC] 1 Mar 2017

Time-optimal problem for redundantly actuated robots moving on a specified path is a challenging problem. Although the problem is well explored and there are proposed solutions based on phase plane analysis, there are still several un-resolved issues regarding calculation of solution curve. In this paper, we explore the characteristics of maximum velocity curve (MVC) and propose an efficient algorithm to establish the solution curve. Then we propose a straightforward method to calculate the maximum/minimum possible acceleration on the path based on the pattern of saturated actuators, which substantially reduces the computational cost. Several numerical examples are provided to illustrate the issues and the solutions.

***Index Terms*—time-optimal, redundantly actuated robots, non-redundant parallel manipulators, robot control.**

I. Introduction

TIME-optimal motion planning remains an ongoing challenge for redundantly actuated robots, such as non-redundant parallel manipulators (NRPM) and humanoid robots during double support phase. While several approaches have been proposed to solve this problem, large computational cost still remains as a major obstacle. We try to propose a computationally efficient algorithm to address the time-optimal problem for redundantly actuated robots.

Several researchers have studied the problem of minimum time motion of manipulators on a specified path for serial and parallel manipulators. In general, there are two approaches, i.e. based on Pontryagin maximum principle and convex optimization to deal with the time-optimal problem of manipulators moving on a specified path. The first method takes advantage of the fact that a system moving on a specified path has only one degree of freedom (DOF). Based on this hypothesis, it is proved that the solution is bang-bang in terms of the acceleration of the tip along the path, $\ddot{s}$. It means the solution curve in $s-\dot{s}$ plane could be obtained by successive integration of the maximum and minimum values of $\ddot{s}$ [1]. Hence, this method is known as numerical integration [2]. Time-optimal problem for both normally and over-actuated robots was solved using numerical integration in [1], [3]–[8] and [9]–[16] respectively.

In convex optimization approach, the time-optimal path tracking problem is transformed into a convex optimal control problem by discretization of s into N segments [17]. Recently, this method has been used to find the minimum time motion of humanoid robots in multi-contact tasks [18]. An advantage of convex optimization method is that its application is not limited to solution of the time-optimal problems, which means that it can equivalently well be used to minimize any other index function. The other advantage of this approach is that there are available commercial packages to solve the convex optimization problem. However, numerical integration method, which directly finds the solution trajectory, has two main advantages which are guaranteed convergence and low computational cost compared with iterative solutions based on convex optimization approach [19]. This paper is focused on integration method and tries to further reduce its computational cost. The goal of this paper is to provide an efficient algorithm to solve the time-optimal problem of redundantly actuated robots moving on a specified path using direct integration method.

In numerical integration method, finding the solution consists of two problems: finding extremum acceleration in each step of solution and extracting switching points. A primary approach to find the extremum acceleration was first proposed in [1] for non-redundant serial manipulators. The admissible range of $\ddot{s}$ is determined at each (s, $\dot{s}$) under actuation constraints. A more rigorous approach to find the maximum or minimum $\ddot{s}$ was proposed in [3] by taking advantages of geometrical concept. In the latter method, inequality constraints on actuators are converted into a convex polygon in $\dot{s}^2-\ddot{s}$ plane. The solution provided in this study, however, was applied in serial robots with no redundant actuators. Recently, this concept has been extended to over-actuated robots based on polytope projection technique [19]. Moreover, linear programming (LP) method is another approach proposed in [9]–[12] to determine extremum acceleration for redundantly actuated system. Due to the fact that LP is a search based algorithm, this method is numerically inefficient. This is the first source of large computation needed to solve the problem.

The second significant problem to obtain the time-optimal solution is how to find switching points in cases that more than one switch exist. Such problems occur when the velocity of the manipulator along the path could exceed a maximum feasible value. In such cases, one needs to establish the maximum velocity curve (MVC) and find possible switching points on

Corresponding author: M.J. Sadigh (email: mjsadigh@ut.ac.ir).

it, which are known as critical points [3]. Hence, constructing MVC plays an important role in finding the critical points. One approach to get MVC is based on searching for the maximum feasible $\dot{s}$ at each point of the path. To this end, one needs to find $\dot{s}$ for which $\ddot{s}_{max} = \ddot{s}_{min}$. This concept is applied for both serial and parallel manipulators in [1] and [9]–[12] respectively. However, it is evident that this method is numerically inefficient due to successive calculation of $\ddot{s}_{max}$ and $\ddot{s}_{min}$ in each step. To reduce computational cost, a method for direct calculation of MVC was suggested in [3] for non-redundant serial manipulators. Recently, the same technique has been used to determine MVC for over-actuated robots [19]. Nevertheless, the construction of MVC for whole domain of s is still costly and numerically expensive.

Among the previous studies, three different strategies are proposed to determine the critical points. The first strategy that theoretically made an important advancement is based on the shooting method [1]. Here, critical points are determined by looking for a solution curve which comes in contact with the MVC without crossing it. However, from practical point of view this approach was very difficult and numerically inefficient. Another strategy which is introduced in [3] determines critical points by comparing the slope of MVC with the slope of solution curve for all point located on MVC. It is evident that in both mentioned strategies, constructing MVC is required which makes the solution computationally expensive. That is why MVC has gained a lot of attention. However, this curve, which is not by itself a solution curve, does not play an important role in finding the switching points. On the other hand, the lower boundary of the trapped area and locked area [4] which are located beneath MVC, plays crucial role in the solution. Indeed this lower boundary which itself is a solution trajectory is the switching curve. All researchers who tried to establish MVC, have used it in their proposed algorithm to construct the switching curve. From this discussion, it is evident that it would be much more efficient if one tries to construct the switching curve directly and skip the step of MVC construction.

To resolve the above-mentioned problem, a straightforward approach was proposed in our previous study [14] to find a subset of critical points, called jump points (known also as zero-inertia points [2], [3], [20]), located on MVC and to establish the switching curve based on that. Such advancement could substantially reduce the computational cost. However, in some cases, which was first encountered in solving the time-optimal problem of humanoid robot during double support phase [15], there remains a part of MVC whose construction is inevitable. This was an important motivation to study such case in more detail and to enhance the method proposed in [14] to solve this type of problems. What makes this study worthwhile is developing the concept of zero-inertia points for redundantly actuated manipulators which could significantly improve the efficiency of the solution algorithm. In this method, we introduce a new strategy to find the critical points by constructing only some parts of MVC that are inevitable. For this, zero-inertia points are obtained analytically and the remaining ones (if any) are determined by calculating the necessary intervals of MVC. This strategy significantly reduces the amount of computation. As explained before, convex polygon of constraints is an essential tool to construct MVC and to determine the saturation pattern of actuators. Construction of this polygon requires considerable amount of computation for over-actuated systems. We developed a new method to convert actuator constraints into a convex polygon in $\dot{s}^2 - \ddot{s}$ plane for over-actuated robots. The proposed method which directly constructs the polygon reduces the computational cost compared with the method proposed in [19] which is based on iteration.

The second issue which is addressed in this paper is how to reduce the computational cost of calculating maximum/minimum acceleration along the path. To this end, we propose a method based on the pattern of saturated actuators to facilitate the calculation of extremum acceleration. The method takes advantage of the fact that the saturation pattern of actuators is preserved in intervals of s. It reduces the challenges of solving LP [9]–[12] or forming polygon [19] at each step of integration to a much simpler problem of finding the pattern of saturated actuators at some specific s and then to solve a linear set of equations of motion at each step.

To summarize, in this study, we tried to improve computational efficiency of solutions based on integration method for minimum time trajectory planning for parallel manipulators with redundant actuators moving on a specified path. To this end, three main contributions are made which are described in section III. In section III-B, a method is proposed for computation of $\ddot{s}_{max}$ and $\ddot{s}_{min}$ which reduces the solution of a linear programming problem, which is to be solved in each step of integration, with solution of a set of linear algebraic equations. In section III-C, we described a novel method to directly establish the convex polygon of constraints, which is essential tool for finding the maximum feasible speed, $\dot{s}_{max}$, for each s. This also reduces computational effort of construction of MVC substantially. The last contribution of this study is described in section III-D in which it is discussed how we may scape construction of MVC, and try to directly establish the solution curve, and which part of MVC needs to constructed, instead of constructing entire of MVC and searching on it for zero-inertia points. The advantage of using these three advancements are shown through solving three examples in section V and comparing the the measured elapsed computation time with the one of presented method in [19]. The results of this comparison are given in section VI.

II. Time Optimal Problem

A special example of redundantly actuated robots is non-redundant parallel manipulators (NRPM) which is considered as object system in this paper. Assume that the NRPM shown in Fig. 1 is supposed to move a payload from an initial point to a final point on a specified path in a minimum time subject to the actuator limits. To state the time-optimal problem let us consider a NRPM composed of v similar, rigid non-redundant serial manipulators working on a single object. The motion of the payload in task space is defined by r coordinates; $\boldsymbol{x} = [x_1, \dots, x_r]^T \in \mathbb{R}^r$ and the motion of the system is defined with n variables, i.e. $\boldsymbol{q} = [q_{11}, \dots, q_{1r}, \dots, q_{v1}, \dots, q_{vr}]^T \in$

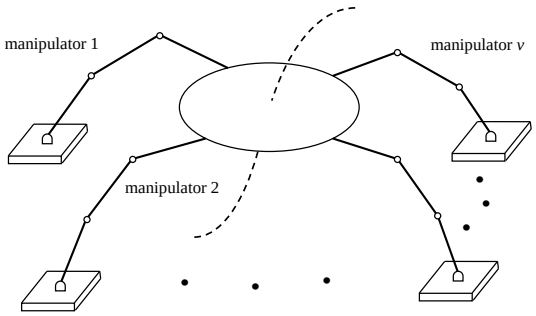

Fig. 1. Schematic diagram for cooperative multi-manipulator system.

$\mathbb{R}^{vr}$ where q_{ij} denotes the jth joint coordinates of the ith manipulator. Due to the kinematic chain configuration, the system is subject to p constraints defined by

$$\phi_i(\boldsymbol{q}) = 0 \qquad i = 1, \dots, p. \tag{1}$$

The equations of motion of such a constrained system can be written as

$$\mathbf{M}(\boldsymbol{q})\ddot{\boldsymbol{q}} + \boldsymbol{h}(\boldsymbol{q}, \dot{\boldsymbol{q}}) + \boldsymbol{g}(\boldsymbol{q}) = \mathbf{B}(\boldsymbol{q})\boldsymbol{\tau} + \mathbf{A}^T\boldsymbol{\lambda} \tag{2}$$

where $\mathbf{M}(\mathbf{q}) \in \mathbb{R}^{n\times n}$ is inertia matrix, $\boldsymbol{h}(\boldsymbol{q}, \dot{\boldsymbol{q}}) \in \mathbb{R}^n$ represents coriolis and centrifugal terms, $\boldsymbol{g}(\boldsymbol{q}) \in \mathbb{R}^n$ indicates gravitational effects, $\mathbf{B}(\boldsymbol{q}) \in \mathbb{R}^{n\times m}$ is actuators coefficient matrix and $\boldsymbol{\tau} \in \mathbb{R}^m$ is input torques. Also, $\boldsymbol{\lambda} \in \mathbb{R}^p$ is Lagrange multipliers and $\mathbf{A} \in \mathbb{R}^{p\times n}$ depicts Jacobian matrix of the constraint equations defined as

$$A_{ij} = \frac{\partial \phi_i}{\partial q_j} \qquad i = 1, \dots, p \qquad j = 1, \dots, n. \tag{3}$$

To eliminate Lagrange multipliers one may premultiply (3) by transpose of orthogonal compliment of $\mathbf{A}$, i.e. matrix $\mathbf{A}^c \in \mathbb{R}^{n\times n-p}$ which satisfies $\mathbf{A}\mathbf{A}^c = 0$. The resulting equations represent a set of $n-p$ new equations with n unknown of $\boldsymbol{q}$ as

$$\overline{\mathbf{M}}(\boldsymbol{q})\ddot{\boldsymbol{q}} + \overline{\boldsymbol{h}}(\boldsymbol{q}, \dot{\boldsymbol{q}}) + \overline{\boldsymbol{g}}(\boldsymbol{q}) = \overline{\mathbf{B}}(\boldsymbol{q})\boldsymbol{\tau} \tag{4}$$

in which $\overline{\mathbf{M}} = \mathbf{A}^{cT}\mathbf{M} \in \mathbb{R}^{n-p\times n}$, $\overline{\boldsymbol{h}} = \mathbf{A}^{cT}\boldsymbol{h} \in \mathbb{R}^{n-p}$, $\overline{\boldsymbol{g}} = \mathbf{A}^{cT}\boldsymbol{g} \in \mathbb{R}^{n-p}$ and $\overline{\mathbf{B}} = \mathbf{A}^{cT}\mathbf{B} \in \mathbb{R}^{n-p\times m}$.

A desired path can be defined by

$$x_i = f_i(s) \qquad i = 1, \dots, r \tag{5}$$

in which x_i is one of the task space coordinates of manipulators and s is an independent non-dimensional parameter that uniquely describes the position of the system along the path. Also, the value of r is equal to $n-p$ due to the fact that each manipulator is kinematically non-redundant.

We may state the time-optimal problem as:

$Problem\ I$: Find the optimum path $\boldsymbol{q}^*(t)$ to minimize the elapsed time $\Gamma = \int_{t_i}^{t_f} dt$ subject to

$$\begin{aligned} &\overline{\mathbf{M}}(\boldsymbol{q})\ddot{\boldsymbol{q}} + \overline{\boldsymbol{h}}(\boldsymbol{q}, \dot{\boldsymbol{q}}) + \overline{\boldsymbol{g}}(\boldsymbol{q}) = \overline{\mathbf{B}}(\boldsymbol{q})\boldsymbol{\tau} \\ &\boldsymbol{x} = \boldsymbol{f}(s) \\ &\boldsymbol{\tau}_{min} \le \boldsymbol{\tau} \le \boldsymbol{\tau}_{max} \end{aligned} \tag{6}$$

with initial and final condition of

$$\begin{aligned} &\boldsymbol{q}(t_i) = \boldsymbol{q}_i, \qquad \dot{\boldsymbol{q}}(t_i) = \dot{\boldsymbol{q}}_i \\ &\boldsymbol{q}(t_f) = \boldsymbol{q}_f, \qquad \dot{\boldsymbol{q}}(t_f) = \dot{\boldsymbol{q}}_f. \end{aligned}$$

To solve $problem\ I$ we restate it in terms of non-dimensional path parameter s. To this end let us define the corresponding task space coordinates in terms of joint coordinates as

$$\boldsymbol{x} = \boldsymbol{p}_i(\boldsymbol{q}_i) \qquad i = 1, \dots, v \tag{7}$$

where $\boldsymbol{q}_i$ and $\boldsymbol{p}_i$ denote the array of joint coordinates of the ith manipulator and direct kinematic relation of $\boldsymbol{x}$. Substituting $\boldsymbol{x}$ from (5) into (7) and solving for $\boldsymbol{q}$ one gets

$$\boldsymbol{q} = \begin{bmatrix} \boldsymbol{q}_1 \\ \vdots \\ \boldsymbol{q}_v \end{bmatrix} = \begin{bmatrix} \boldsymbol{p}_1^{-1}(\boldsymbol{f}(s)) \\ \vdots \\ \boldsymbol{p}_v^{-1}(\boldsymbol{f}(s)) \end{bmatrix} = \boldsymbol{q}(s). \tag{8}$$

Differentiating (8), $\dot{\boldsymbol{q}}$ and $\ddot{\boldsymbol{q}}$ are calculated as

$$\dot{\boldsymbol{q}} = \boldsymbol{q}'(s)\dot{s} \tag{9}$$

and

$$\ddot{\boldsymbol{q}} = \boldsymbol{q}'(s)\ddot{s} + \boldsymbol{q}''(s)\dot{s}^2 \tag{10}$$

in which $(.)'$ and $(.)''$ denotes first and second derivative with respect to s. Plugging these relations into (4), equations of motion can be written as

$$\overline{\boldsymbol{c}}(s)\ddot{s} + \overline{\boldsymbol{d}}(s)\dot{s}^2 + \overline{\boldsymbol{e}}(s) = \overline{\mathbf{B}}(s)\boldsymbol{\tau} \tag{11}$$

where

$$\begin{aligned} &\overline{\boldsymbol{c}}(s) = \overline{\mathbf{M}}(\boldsymbol{q}(s))\boldsymbol{q}'(s) \\ &\overline{\boldsymbol{d}}(s) = \overline{\mathbf{M}}(\boldsymbol{q}(s))\boldsymbol{q}''(s) + \overline{\boldsymbol{h}}(\boldsymbol{q}(s), \boldsymbol{q}'(s)) \\ &\overline{\boldsymbol{e}}(s) = \overline{\boldsymbol{g}}(\boldsymbol{q}(s)) \end{aligned} \tag{12}$$

in which all $\overline{\boldsymbol{c}}$, $\overline{\boldsymbol{d}}$ and $\overline{\boldsymbol{e}}$ are member of $\mathbb{R}^{n-p}$.

The relation 11 represents $n-p$ equations with two states $[s, \dot{s}]$. Any motion of the system which follows the prescribed path must satisfy all above $n-p$ equations. Now, the optimization problem can be rewritten as:

$Problem\ II$: Find the optimum path $s^*(t)$ to minimize the elapsed time $\Gamma = \int_{t_i}^{t_f} dt$ subject to

$$\begin{aligned} &\overline{\boldsymbol{c}}(s)\ddot{s} + \overline{\boldsymbol{d}}(s)\dot{s}^2 + \overline{\boldsymbol{e}}(s) = \overline{\mathbf{B}}(s)\boldsymbol{\tau} \\ &\boldsymbol{\tau}_{min} \le \boldsymbol{\tau} \le \boldsymbol{\tau}_{max} \end{aligned} \tag{13}$$

with initial and final condition of

$$\begin{aligned} &s(t_i) = 0, \qquad \dot{s}(t_i) = \dot{s}_i \\ &s(t_f) = 1, \qquad \dot{s}(t_f) = \dot{s}_f. \end{aligned}$$

As we stated earlier in introduction, finding the solution of $problem\ II$ is equivalent to solve two major problems of finding extremum acceleration and extracting switching points. In the next section, after a detailed review of some background, we propose an efficient method to calculate the extremum acceleration based on pattern of saturated actuators.

III. Optimization Method

A. Background: Linear Programming Approach

Overall form of the $problem\ II$ resembles that of the time-optimal for non-redundant serial manipulators. Actuators coefficient matrix, $\overline{\mathbf{B}}(s)$, is an invertible square matrix for normally actuated robots, which could be transformed into a unique matrix by appropriate selection of generalized coordinates. By doing so, only one actuator appears in each motion equation. The solution method of [1] and [3], which was used to solve the time-optimal problem of non-redundant serial manipulators, is based on the same thing. For NRPM which has redundancy in actuators, $\overline{\mathbf{B}}(s)$ is a non-square matrix. That is why more than one actuator appears in each motion equation. For solving the time-optimal problem of NRPM, hence, provided methods for serial manipulators cannot be used. This issue was independently addressed in [9] and [10] where the problem of finding extremum acceleration was introduced as:

$Problem\ III$: Find $\boldsymbol{\tau}$ to maximize or minimize $\ddot{s}$ subject to

$$\begin{aligned} &\overline{\boldsymbol{c}}(s)\ddot{s} + \overline{\boldsymbol{d}}(s)\dot{s}^2 + \overline{\boldsymbol{e}}(s) = \overline{\mathbf{B}}(s)\boldsymbol{\tau} \\ &\boldsymbol{\tau}_{min} \leq \boldsymbol{\tau} \leq \boldsymbol{\tau}_{max}. \end{aligned} \tag{14}$$

Solving this problem is equivalent to a linear programming (LP) strategy to find minimum or maximum acceleration. In order to acquire the solution, the problem must be solved for each s. Acceleration along the path, $\ddot{s}$, can be calculated by premultiplying (11) by $\overline{\boldsymbol{c}}^T$ as

$$\ddot{s} = \frac{1}{\overline{\boldsymbol{c}}^T\overline{\boldsymbol{c}}}(\overline{\boldsymbol{c}}^T\overline{\mathbf{B}}\boldsymbol{\tau} - \overline{\boldsymbol{c}}^T\overline{\boldsymbol{d}}\dot{s}^2 - \overline{\boldsymbol{c}}^T\overline{\boldsymbol{e}}). \tag{15}$$

For above acceleration can hold the robot on the path, all $n-p$ equations of the (11) must be satisfied. That is to say, for minimizing or maximizing the acceleration from the (15), $n-p-1$ equations of (16), which are obtained prior to premultiplying (11) by transpose of orthogonal complement matrix of the vector $\overline{\boldsymbol{c}}^T$, $(\overline{\boldsymbol{c}}^T)^{c^T} \in \mathbb{R}^{n-p-1\times n-p}$, must be fulfilled as constraints

$$\boldsymbol{d}'\dot{s}^2 + \boldsymbol{e}' = \mathbf{B}'_{n-p-1\times m}\boldsymbol{\tau} \tag{16}$$

in which $\boldsymbol{d}' = (\overline{\boldsymbol{c}}^T)^{c^T}\overline{\boldsymbol{d}} \in \mathbb{R}^{n-p-1}$, $\boldsymbol{e}' = (\overline{\boldsymbol{c}}^T)^{c^T}\overline{\boldsymbol{e}} \in \mathbb{R}^{n-p-1}$ and $\mathbf{B}' = (\overline{\boldsymbol{c}}^T)^{c^T}\overline{\mathbf{B}} \in \mathbb{R}^{n-p-1\times m}$.

Therefore the problem of determining maximum or minimum acceleration, $problem\ III$, becomes as:

$Problem\ IV$: Find $\boldsymbol{\tau}$ to maximize or minimize $\ddot{s} = \frac{1}{\overline{\boldsymbol{c}}^T\overline{\boldsymbol{c}}}(\overline{\boldsymbol{c}}^T\overline{\mathbf{B}}\boldsymbol{\tau} - \overline{\boldsymbol{c}}^T\overline{\boldsymbol{d}}\dot{s}^2 - \overline{\boldsymbol{c}}^T\overline{\boldsymbol{e}})$ subject to

$$\begin{aligned} &\boldsymbol{d}'\dot{s}^2 + \boldsymbol{e}' = \mathbf{B}'\boldsymbol{\tau} \\ &\boldsymbol{\tau}_{min} \leq \boldsymbol{\tau} \leq \boldsymbol{\tau}_{max}. \end{aligned} \tag{17}$$

It is demonstrated in [13] that for a robotic system with n generalized coordinates, p holonomic constraints and m actuators, at least $m-n+p+1$ actuators are in saturated state. This property is expressed in this way that because the above problem has $n-p-1$ equal constraints, $n-p-1$ actuators can be calculated by other $m-(n-p-1)$ actuators. Therefore, solving the $problem\ IV$ is equivalent to a linear programming (LP) strategy to find $m-n+p+1$ saturated actuators which lead to $\ddot{s}$ being maximized or minimized. In order to determine the solution, LP should be executed for calculation of extremum acceleration in each step. Hence, due to the fact that LP is a search based algorithm, this method requires high amount of calculations. To overcome this problem, we introduce a method based on the saturation pattern of actuators in next section.

B. Saturation Pattern of Actuators

Considering the fact that when $\ddot{s}$ accepts its extremum, at least $m-n+p+1$ actuators are saturated [13], one can easily compute non-saturated actuators and $\ddot{s}$ from (11). To this end, we write

$$\overline{\boldsymbol{c}}(s)\ddot{s} + \overline{\boldsymbol{d}}(s)\dot{s}^2 + \overline{\boldsymbol{e}}(s) = \begin{bmatrix}\overline{\mathbf{B}}_{ns} & \overline{\mathbf{B}}_s\end{bmatrix}\begin{bmatrix}\boldsymbol{\tau}_{ns} \\ \boldsymbol{\tau}_s\end{bmatrix} \tag{18}$$

in which $\boldsymbol{\tau}_{ns} \in \mathbb{R}^{n-p-1}$ and $\boldsymbol{\tau}_s \in \mathbb{R}^{m-n+p+1}$.

For every point along the solution path, one can always be found a neighborhood in which saturation pattern of actuators does not change. Therefore, we may use a set of saturated actuators at one point to calculate $\ddot{s}$ and $\boldsymbol{\tau}_{ns}$ for other points in its neighborhood. So the problem of determining extremum acceleration, $problem\ IV$, reduces to:

$Problem\ V$: Assuming $\boldsymbol{\tau}_s$ to be known, find $\boldsymbol{\tau}_{ns}$ and $\ddot{s}$ from

$$\begin{bmatrix}\overline{\boldsymbol{c}}(s) & -\overline{\mathbf{B}}_{ns}\end{bmatrix}\begin{bmatrix}\ddot{s} \\ \boldsymbol{\tau}_{ns}\end{bmatrix} = -\overline{\boldsymbol{d}}(s)\dot{s}^2 - \overline{\boldsymbol{e}}(s) + \overline{\mathbf{B}}_s\boldsymbol{\tau}_s. \tag{19}$$

Clearly solution of (19), which is a linear set is much easier and involves less computation compared with (17) which is a linear programming problem. To solve the problem at hand, first, the saturated actuators set which leads to maximization or minimization of acceleration is determined by constructing the polygon of constraints in $\dot{s}^2 - \ddot{s}$ plane for the starting point, see section III-C for details. Then, from (19) values of $\ddot{s}$ and $\boldsymbol{\tau}_{ns}$ are calculated and based on the equations of motion are integrated to find the next values of s and $\dot{s}$. Hence we assume that the saturated actuators remain saturated and based on this assumption compute $\boldsymbol{\tau}_{ns}$ from (19). If non of these values exceed actuator bound we may proceed to next step. But, if at least one of the values of $\boldsymbol{\tau}_{ns}$ exceeds its bound it means that the pattern of saturation is changed and we need to establish the polygon to find real set of saturated actuators. Fig. 2 shows the flow diagram of the proposed algorithm which we call it SPA hereafter.

By applying this innovative method, while the $problem\ V$ is solved in each integration step, determining the pattern of saturated actuators which is more complicated, is done

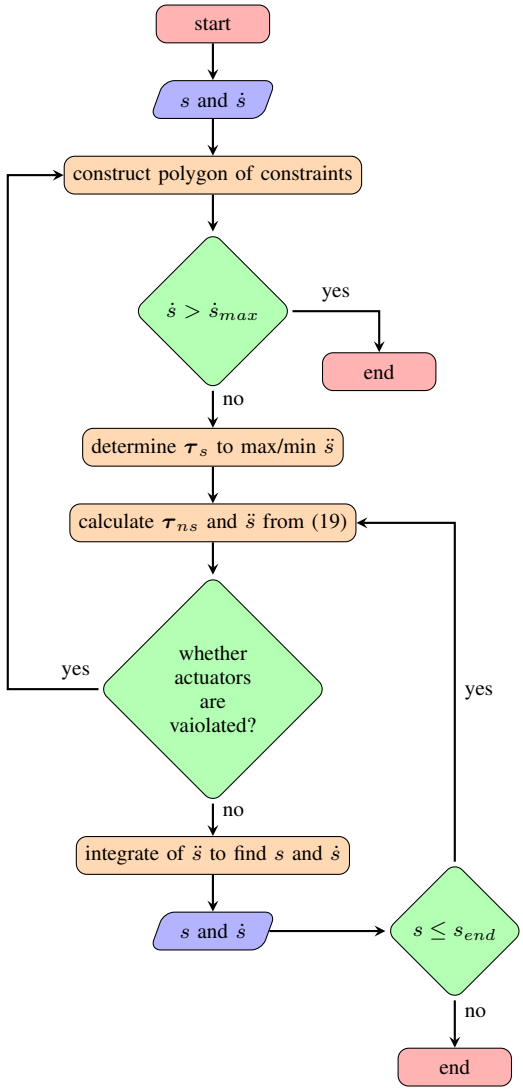

Fig. 2. Flow diagram of the SPA strategy

only in some limited points, where pattern of saturation is changed. This method, hence, significantly reduces the amount of computation.

C. Polygon of Constraints

As mentioned in previous section, there are points on the path for which we need to find $\dot{s}_{max}$ or $\dot{s}_{min}$ and the pattern of saturation of actuators. In addition to that one might also need to find the maximum possible $\dot{s}$ at each s to establish MVC. One efficient method to solve both of the above mentioned problems is to establish polygon of constraints which first reported in [3] for serial manipulators.

To construct the polygon for NRPM system, we attempt to extend the method proposed in [3]. For this, consider relation (11) which contains $n-p$ equations. Choosing $n-p$ independent actuators $\boldsymbol{\tau}_a \in \mathbb{R}^{n-p}$, one might rewrite relation (11) as

$$\overline{\boldsymbol{c}}(s)\ddot{s} + \overline{\boldsymbol{d}}(s)\dot{s}^2 + \overline{\boldsymbol{e}}(s) = \begin{bmatrix}\overline{\mathbf{B}}_a & \overline{\mathbf{B}}_b\end{bmatrix}\begin{bmatrix}\boldsymbol{\tau}_a \\ \boldsymbol{\tau}_b\end{bmatrix}. \qquad (20)$$

in which $\boldsymbol{\tau}_b \in \mathbb{R}^{m-n+p}$ is the remaining actuators. Premultiplying (20) by ${\overline{\mathbf{B}}_a}^{-1}$ leads to

$$\overline{\overline{\boldsymbol{c}}}(s)\ddot{s} + \overline{\overline{\boldsymbol{d}}}(s)\dot{s}^2 + \overline{\overline{\boldsymbol{e}}}(s) = \boldsymbol{\tau}_a + \overline{\overline{\mathbf{B}}}\boldsymbol{\tau}_b = \boldsymbol{\tau}' \qquad (21)$$

in which $\overline{\overline{\boldsymbol{c}}} = {\overline{\mathbf{B}}_a}^{-1}\overline{\boldsymbol{c}} \in \mathbb{R}^{n-p}$, $\overline{\overline{\boldsymbol{d}}} = {\overline{\mathbf{B}}_a}^{-1}\overline{\boldsymbol{d}} \in \mathbb{R}^{n-p}$, $\overline{\overline{\boldsymbol{e}}} = {\overline{\mathbf{B}}_a}^{-1}\overline{\boldsymbol{e}} \in \mathbb{R}^{n-p}$ and $\overline{\overline{\mathbf{B}}} = {\overline{\mathbf{B}}_a}^{-1}\overline{\mathbf{B}}_b \in \mathbb{R}^{n-p\times m-n+p}$. One should note that existence of ${\overline{\mathbf{B}}_a}^{-1}$ is guaranteed by the virtue of independency of actuators $\boldsymbol{\tau}_a$.

In any equation of (21), all $\boldsymbol{\tau}_b$ and one of τ_{ai}, which equal to $m-(n-p)+1$ actuators, appear. By selecting the appropriate values of $\boldsymbol{\tau}_b$ and τ_{a_i} from their lower or upper bound, one could obtain the minimum and maximum values for τ_i'. Therefore, each equation of (21) shows two straight lines on the plane $\dot{s}^2 - \ddot{s}$. The area out of these two lines indicates a region in which for any $(\dot{s}^2, \ddot{s})$ and given τ_{a_i} in its limitation bound, one of $\boldsymbol{\tau}_b$ actuators is certainly out of saturation bound. The feasible area, hence, is restricted to points between these two lines. For any state of choosing $\boldsymbol{\tau}_b$ and considering all equations of (21), there are $n-p$ pairs of lines which constitute a polygon on the plane $\dot{s}^2 - \ddot{s}$. For any $(\dot{s}^2, \ddot{s})$ outside the polygon and given an admissible $\boldsymbol{\tau}_a$, one of $\boldsymbol{\tau}_b$ actuators is definitely out of saturation bound. The feasible area is restricted to points into this polygon. However, All of points in this polygon are not acceptable and all states of choosing $\boldsymbol{\tau}_b$ need to be checked. The common areas of these polygons are considered as feasible areas of NRPM. This area constitutes a unique polygon which is the same as the one established for serial manipulators [3].

The polygon constructed for NRPM is the common area restricted by $C(m, m-(n-p)) \times n-p$ pairs of line (C is combination function). For any given $(\dot{s}^2, \ddot{s})$ inside the polygon, there is one feasible $\boldsymbol{\tau}$ that satisfies the actuators saturation limits. On the edge of polygon, $m-(n-p)+1$ actuators are in saturation bound of which, $m-(n-p)$ are those of $\boldsymbol{\tau}_b$ and the other one is one of the corresponding $\boldsymbol{\tau}_a$. At any vertex of polygon at least $m-(n-p)+2$ actuators are in saturation bound. The set of saturated actuators on each edge is the common ones at two vertices located at the ends of the edge. Therefore, by knowing the saturated actuators at vertices of polygon, the pattern of saturation on each edge is determined.

In this paper, we develop a new method to establish the polygon for NRPM by finding its vertices. By applying this method, in addition to the position of vertices in $\dot{s}^2 - \ddot{s}$ plane, the set of saturated actuators at each vertex is also obtained. Our proposed strategy to construct the polygon is as follows:

i. Choose a state of $\boldsymbol{\tau}_b$ and extract relation (21) for it.
ii. For each equation of (21), establish the corresponding pair of lines on $\dot{s}^2 - \ddot{s}$ plane.
iii. Calculate all intersection points of each two lines which has the same value of $\boldsymbol{\tau}_b$.
iv. For each intersection points, compute the value of $\boldsymbol{\tau}_a$ form (21) and check whether $\boldsymbol{\tau}_a$ is in its bound or not. If not, this point could not be a vertex of polygon and should be ignored.

v. Continue step i to iv until all possible states of $\boldsymbol{\tau}_b$ are selected. After this, all vertices of the polygon are obtained.

The developed method is a straightforward and efficient strategy to find the polygon. It is different from the approach proposed in [19] that is based on polytope projection technique. This technique iteratively attempts to find polygon by expanding the edges which leads to a trade-off between accuracy and computational cost.

D. Critical Points

An important step to find the solution is determining the points to switch between minimum and maximum acceleration. For this purpose, the first stage is calculating the critical points which are candidate for switching points on the MVC. The concept of critical points was first introduced in [3]. Points on the MVC are categorized as sink or source depending on whether the slope of solution curve in phase plane, $\ddot{s}/\dot{s}$, is greater or smaller than the slope of the MVC, k'. Any solution starting from a source continues in feasible region, whereas any solution starting from a sink immediately leaves the feasible region. The critical points are by definition ones that the MVC change from sink to source.

In this section, we propose an intelligent strategy to find the critical points by improving our previous study [14]. This strategy generally involves two steps. The first step is analytically determining zero-inertia points for over-actuated robots. In [14], we showed that zero-inertia points might happen where one of $\overline{\overline{c}}_i(s)$ in (21) vanishes. These points can be directly calculated using

$$\overline{\overline{c}}_i(s^\dagger) = 0. \tag{22}$$

However, each of $s^\dagger$ does not indicate a zero-inertia point. To check this, the polygon should be constructed for each $s^\dagger$ to see whether the most right edge of polygon is vertical or not. If not, this $s^\dagger$ is not passable and should be ignored. For acceptable ones, the maximum velocity of the corresponding polygon is considered as $\dot{s}^\dagger$ for zero-inertia point.

One should note that not all zero-inertia points located on the MVC are candidates for switching points. There are four possible situations for a zero-inertia point. The characteristic of the boundary on each point may change from sink to source or source to sink. Whereas the nature of points on the boundary may not change, i.e. points on both sides are sink and on both sides source. Out of these, only zero-inertia points are of the sink–source type critical points. To realize the type of a zero-inertia point without constructing the MVC, one needs to establish the solution from such points in backward and forward direction with $\ddot{s}_{min}$ and $\ddot{s}_{max}$ respectively. It is done by executing the SPA strategy proposed in section III-B. If the zero-inertia point is of the sink–sink type, for forward direction the actuators bound immediately are violated which means that forward path instantly enters the non-feasible region (NFR). Also, if the point is of the source–source type, the actuators limit immediately are violated for backward direction. Similarly, if the point is of the source–sink type for both the forward and backward direction actuators bound are broken immediately.

In some cases, the solution is fully obtained by knowing zero-inertia points. However, logically one might think of a critical point which is not a zero-inertia point, see [15]. Characteristics of the MVC on such point smoothly changes from sink to source. In such cases determining only zero-inertia points would lead to an incomplete solution. The second step of our strategy is determining some of smooth critical points which complete the solution. For this, the MVC is constructed for intervals of s which is uncovered by the solution generated from zero-inertia points. Then, by calculating $\ddot{s}/\dot{s}-k'$ for these intervals the remaining critical points are determined. These points are candidate of the other switching location on the MVC which are used to form the last portions of the solution.

In the developed strategy, in order to determine the switching points, only some parts of the MVC are constructed. It is more efficient than the other studies, e.g. [19], which establish MVC in the whole domain of s.

IV. Solution Algorithm

In this section, we provide an efficient algorithm to solve the time-optimal problem of redundantly actuated robots moving on a specified path. The algorithm utilizes strategies introduced in previous sections to find critical points and determine the pattern of saturated actuators. In phase plane the higher solution trajectory has the shorter traveling time. By considering this fact, we propose the following algorithm to find the time-optimal trajectory:

$Step\ 1$: Execute SPA strategy by starting from initial point, $D_i(0, \dot{s}_i)$, in forward direction with $\ddot{s}_{max}$. Similarly, execute SPA strategy by starting from final point, $D_f(1, \dot{s}_f)$, in backward direction with $\ddot{s}_{min}$. Continue these two procedures until either the line of $s = 0$ or $s = 1$ is crossed or actuators bound are violated, i.e. solution trajectories enter the NFR (points b_i and b_f in Fig. 3). If one or both of the curves intersects the line of $s = 0$ or $s = 1$, solution trajectories cross each other at feasible region (FR). Therefore, the algorithm ends and the solution curve is obtained with one switching point. Otherwise, zero-inertia points should be determined, like the case shown in Fig. 3.

$Step\ 2$: Apply the strategy proposed in section III-D to calculate a set of zero-inertia points with the type of sink–source which are located on MVC between b_i and b_f, e.g. C_2 and C_3 in Fig. 3. If there is no such points skip to $Step\ 6$.

$Step\ 3$: Execute SPA strategy by starting from the lowest point of the set, C_2, in backward and forward direction with $\ddot{s}_{min}$ and $\ddot{s}_{max}$ respectively. This process is continued until either the solution trajectories generated in previous steps is crossed (S_1) or no acceptable solution fulfills the actuators limits (point b_2 on MVC).

$Step\ 4$: Ignore all other points of the set, C_3, which are located above the generated solution curve inside an inadmissible area, i.e. trapped and locked area which introduced in [4].

$Step\ 5$: Repeat $Steps\ 3$ and 4 from the lowest remaining points of the set. Continue the same process for other points

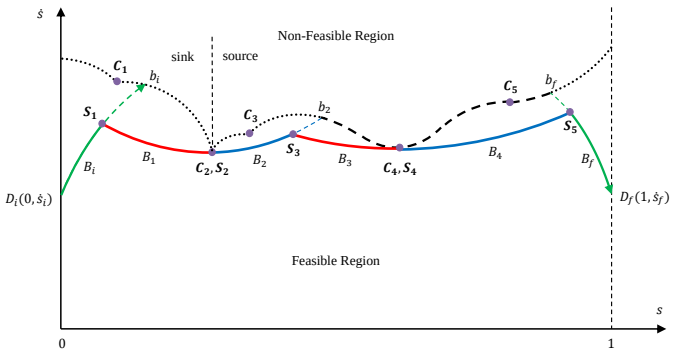

Fig. 3. Schematic diagram of the construction of the solution curve. In this figure, D_i and D_f are initial and final points of solution curve, C_j is jth critical point, S_j is jth switching point, B_i and B_f are initial and final branches of solution curve, B_j is jth branch of solution curve, b_i and b_f are points that initial and final solution curves enter NFR, and b_j is point that jth solution curve enters NFR.

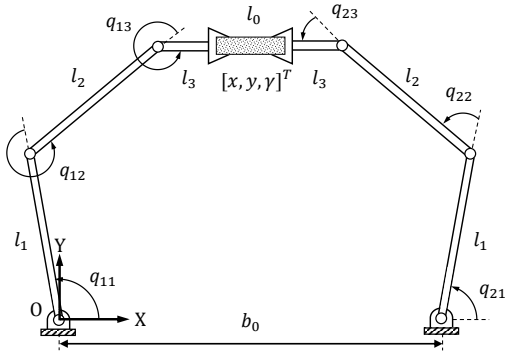

Fig. 4. The planar NRPM.

TABLE I
PHYSICAL CHARACTERISTICS OF THE SYSTEM

Length (m)		Mass (kg)	
l_0	0.2	m_0	1
l_1	0.5	m_1	1
l_2	0.6	m_2	1
l_3	0.3	m_3	0.3
b_0	1.4		

Limit Torques (N.m)
$\boldsymbol{\tau}_{limit} = \pm[35, 25, 10, 35, 25, 10]^T$

of the set until either the generated solution curve covers the whole domain of s from 0 to 1 or there remains no zero-inertia point outside trapped and locked area, like the case shown in Fig. 3. If both of the initial and final solution trajectories which are established in $Step$ 1 are crossed with the generated curve, the algorithm ends and the solution curve is obtained. Otherwise, some parts of MVC should be constructed, like the case shown in Fig. 3.

$Step$ 6 : Construct portions of MVC which are not covered by previously generated solution curve, i.e. dashed curve $b_2 b_f$. It is done by establishing polygons for such intervals using the algorithm proposed in section III-C.

$Step$ 7 : By calculating $\ddot{s}/\dot{s} - k'$, find a set of smooth critical points where the characteristics of the MVC constructed in $Step$ 6 changes from sink to source, e.g. points C_4 and C_5.

$Step$ 8 : Repeat $Step$ 5 for the set of smooth critical points to obtain the last portions of solution curve, i.e. B_3 and B_4 trajectories. After doing this, lowest portions of solution curves B_1 to B_n constitute the solution curve, e.g. curve $D_i S_1 C_2 S_3 C_4 S_5 D_f$ in Fig. 3.

A switching point located on MVC could be either smooth critical point or zero-inertia point. By executing the proposed algorithm, depending on the variety of switching points, three general cases may happen which we call them indirect, direct and semi-direct procedures. When there is no zero-inertia points on MVC the procedure is indirect. In this case, all of the switching points are determined by constructing a portion of MVC which is not covered by initial and final solution curves generated in $Step$ 1. Direct procedure happens when all of the switching points are zero-inertia points. In this case, without constructing any part of MVC the solution curve is calculated directly. Semi-direct procedure occurs when switching points are the combination of smooth critical points and zero-inertia points. In this case, the solution is obtained by constructing some portions of MVC which are uncovered by generated solution from zero-inertia points in $Step$ 5. In the next section, to clarify the developed solution algorithm, three examples are given to represent each of the cases.

V. NUMERICAL EXAMPLE

In this section, three numerical examples are presented to solve the time-optimal problem of NRPM to track a specified path. For this end, we consider two different NRPM systems which one of them is planar and the other is three dimensional. The first and second examples are given for the planar NRPM with different motion paths that show the semi-direct and direct procedures respectively. The third example illustrates an indirect procedure to solve the time-optimal problem for 3D NRPM which clearly shows the effectiveness and efficiency of the proposed algorithm.

A. Example I: Semi-Direct Procedure

Fig. 4 shows the schematic of a NRPM composed of two planar manipulators handling a payload. Each manipulator has 3 DOFs which rigidly grasped a payload such that no slipping or rotation is possible at contact points. For this system $n = 6$, $p = 3$ and $m = 6$. The physical properties of the system are listed in Table I. The system is assumed to move the payload on a prescribed path defined as

$$\begin{cases} x(s) = 0.6(s - 0.5) + 0.7 \\ y(s) = -3.46s^5 + 8.66s^4 - 5.77s^3 + 0.58s + 0.7 \\ \gamma(s) = -0.45(s - 0.5) \end{cases} \tag{23}$$

with $\dot{s}_i = 4$ and $\dot{s}_f = 4$.

The procedure begins by executing SPA strategy in forward direction by starting from initial point, $D_i(0, 4)$, which results branch B_i, as shown in Fig. 5a. The solution is continued by performing the same strategy in backward direction by

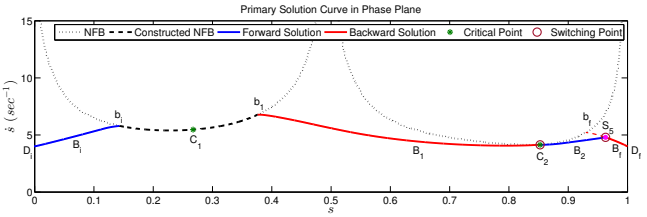

(a) Primary solution curve

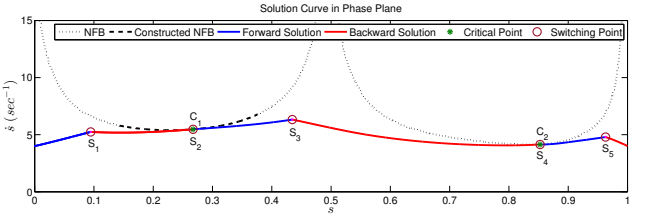

(b) Final solution curve

Fig. 5. The solution curve, critical and switching points calculated for semi-direct procedure (example I).

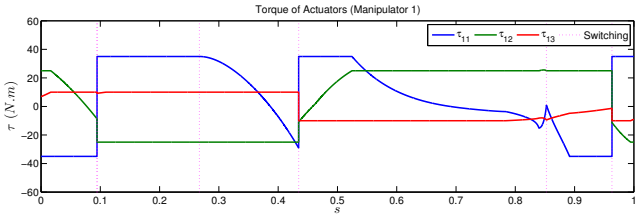

(a) Manipulator 1

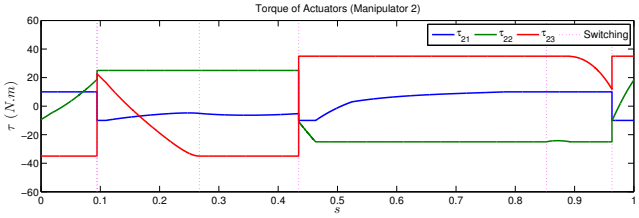

(b) Manipulator 2

Fig. 6. Actuator torques calculated for semi-direct procedure (example I).

starting from final point, D_f(1, 4), which makes branch B_f. Actuators bound are violated at b_i(0.1434, 5.7960) and b_f(0.9301, 5.2179) that means the solution enters NFR at these points. By following the solution algorithm, the only zero-inertia point is calculated as C_2(0.8526, 4.1395). Then, SPA strategy is applied in backward and forward direction by starting from C_2 that makes branches B_1 and B_2. When the branch B_1 reaches to b_1(0.3758, 6.7744) the actuators limit are broken. Also, branch B_2 crosses the curve B_f at S_5(0.9630, 4.7920).

The solution curve is unknown between b_i and b_1. Therefore, to complete the solution, a portion of MVC which is not covered by the generated solution curve is constructed. This part of MVC is shown with dashed curve in Fig. 5a. One should note that portions of MVC shown in Fig. 5a by dotted line are not necessary for calculating of the solution curve and are drawn only for better understanding.

Values of $\ddot{s}/\dot{s}$ and slope of MVC are compared to categorize points on MVC as sink or source. The behavior of the MVC changes smoothly from sink to source at $s_{c_1} = 0.2672$. To obtain the solution curve, we execute SPA strategy by starting from C_1, forwardly with $\ddot{s}_{max}$ and backwardly with $\ddot{s}_{min}$ respectively, up to the point where generated solution curve in previous steps is crossed in S_1(0.0945, 5.2431) and S_3(0.4345, 6.3232). The solution curve has been shown in Fig. 5b. The minimum time calculated, also, amounts to 0.206 sec.

The solution curve includes five switching points of S_1(0.0945, 5.2431), S_2(0.2672, 5.4703), S_3(0.4345, 6.3232), S_4(0.8526, 4.1395) and S_5(0.9630, 4.7920). Points S_1, S_3 and S_5 are located out of MVC and the acceleration is switched from the maximum value to its minimum. However, two other switching points, S_2 and S_4, are placed on MVC and the acceleration is switched from the minimum value to its maximum. At both critical points, the acceleration changes continuously from minimum value to its maximum. However, the acceleration is discontinuous at the switching points which are located out of MVC. Fig. 6 shows the actuator torques of each robot arms while moving on the prescribed path with the minimum time solution. In terms of continuity, the actuator torques has the same behavior of the acceleration at switching points. Also, the torque limitation has been fulfilled and on each point of the path, at least four actuators are always saturated.

B. Example II: Direct Procedure

The NRPM system considered in this example is similar to the one introduced in section V-A. To show the effect of payload path on the procedure of finding the solution curve, a different path is defined as

$$\begin{cases} x(s) = 0.2\ cos(2\pi s) + 0.7 \\ y(s) = 0.2\ sin(2\pi s) + 0.62 \\ \gamma(s) = 0.7\ s \end{cases} \tag{24}$$

with $\dot{s}_i = 0$ and $\dot{s}_f = 0$.

Based on the solution algorithm, the procedure begins by executing SPA strategy in forward and backward direction by starting from (0, 0) and (1, 0) respectively which results the initial and final solution curves, as shown in Fig. 7. By following the solution algorithm, five zero-inertia points are calculated as C_1(0.5776, 1.9478), C_2(0.6936, 2.3730), C_3(0.8714, 2.3583), C_4(0.9336, 2.4464) and C_5(0.9910, 2.4535). Points C_4 and C_5 covered by the final solution curve are eliminated from the set of zero-inertia points. Then, SPA strategy is applied in backward and forward direction by starting from C_1 which lead to point C_2 is placed on locked area. Hence, this point can not be a candidate for a switching point. The other portions of solution curve are found by executing the same strategy in forward and backward direction by starting from the last remaining zero-inertia point, C_3. The generated curves cover whole domain of s from 0 to 1 and the solution algorithm ends without constructing any part of MVC. The solution curve consists of five switching points S_1(0.2536, 3.0889), S_2(0.5776, 1.9478), S_3(0.7628, 2.4767), S_4(0.8714,

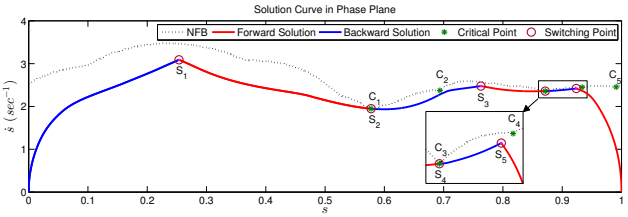

Fig. 7. The solution curve, critical and switching points calculated for direct procedure (example II).

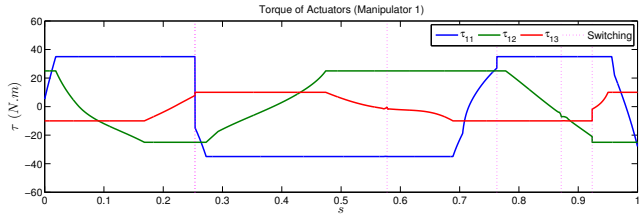

(a) Manipulator 1

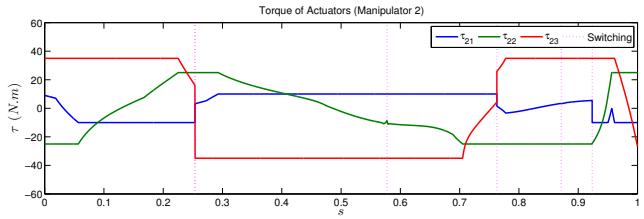

(b) Manipulator 2

Fig. 8. Actuator torques calculated for direct procedure (example II).

2.3583) and S_5(0.9236, 2.4187) as shown in Fig. 7. The minimum time calculated, also, amounts to 0.478 sec. Fig. 8 shows the actuator torques of each robot arms while moving the prescribed path with the time-optimal solution. The torque limitation has been fulfilled and on each point of the path, at least four actuators are always saturated.

C. Example III: Indirect Procedure

The NRPM system considered at this example is composed of two PUMA 560 manipulators which are handling a payload. Each manipulator has 6 DOFs which rigidly grasped a payload such that no slipping or rotation is possible at contact points. For this system $n = 12$, $p = 6$ and $m = 12$. The physical characteristics and Denavit-Hartenberg parameters of PUMA 560 are listed in Table II. The system is assumed to move the payload on a prescribed path defined as

$$\begin{cases} x(s) = 0.2\ cos(2\pi s) + 0.77 \\ y(s) = 0.15\ sin(2\pi s) + 0.122 \\ z(s) = 0.1\ cos(2\pi s) - 0.1 \\ \alpha(s) = \frac{\pi}{8}\ sin(2\pi s) \\ \beta(s) = \frac{\pi}{3}\ sin(2\pi s) + \frac{\pi}{2} \\ \gamma(s) = \frac{\pi}{12}\ sin(2\pi s) + \frac{\pi}{6} \end{cases} \tag{25}$$

with $\dot{s}_i = 1$ and $\dot{s}_f = 1$.

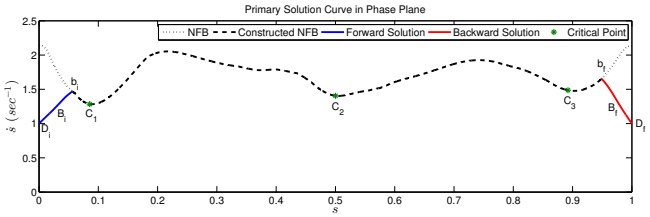

(a) Primary solution curve

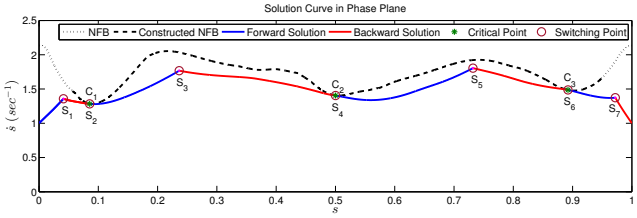

(b) Final solution curve

Fig. 9. The solution curve, critical and switching points calculated for indirect procedure (example III).

The procedure begins by executing SPA strategy in forward and backward direction from D_i(0, 1) and D_f(1, 1) respectively which results in branches B_i and B_f, as shown in Fig. 9a. Actuators bound are violated at b_i(0.0564, 1.4694) and b_f(0.9488, 1.6534) that means the solution enters NFR at these points. In the range of $b_i b_f$ there is no zero-inertia point of the sink-source type. Thereby to generate the solution, a portion of MVC placed between b_i and b_f is constructed. This part of MVC is shown with dashed curve in Fig. 9a.

To determine smooth critical points values of $\ddot{s}/\dot{s}$ and slope of MVC are compared. The behavior of the MVC changes smoothly from sink to source at points $s_{c_1} = 0.0854$, $s_{c_2} = 0.5001$ and $s_{c_3} = 0.8922$. The solution curves are established by performing SPA strategy in backward and forward direction by starting from points C_1, C_2 and C_3 respectively. The generated curves cover whole domain of s from 0 to 1 and the solution algorithm ends. The solution curve consists of seven switching points S_1(0.0412, 1.3573), S_2(0.0854, 1.2833), S_3(0.2365, 1.7672), S_4(0.5001, 1.4047), S_5(0.7319, 1.8045), S_6(0.8922, 1.4868) and S_7(0.9720, 1.3734) as shown in Fig. 9b. The minimum time calculated, also, amounts to 0.674 sec. The actuator torques of each robot arms for the minimum time solution is shown in Fig. 10. The torque limitation has been fulfilled on each point of the path and at least seven actuators are always located in their saturation bound.

The importance of using an efficient algorithm to compute the minimum time solution is more clear in *Example III*. It can be investigated in two different aspects. First, the NRPM system which is composed of two PUMA 560 manipulators is more complicated than planar robot considered in two previous examples. Second, for the path prescribed in (25), there is no zero-inertia point, therefore, to determine the critical points, a large portion of MVC should be constructed.

TABLE II
DENAVIT-HARTENBERG PARAMETERS AND PHYSICAL CHARACTERISTICS OF PUMA 560 [21]

i	α_{i-1}	A_{i-1}	D_i	$m_i(kg)$	$\boldsymbol{s}_i(mm)$			$\boldsymbol{I}_i(kg.m^2)$		
					s_{x_i}	s_{y_i}	s_{z_i}	I_{xx_i}	I_{yy_i}	I_{zz_i}
1	0	0	0	-	-	-	-	-	-	0.35
2	-90	0	243.5	17.40	68	6	-16	130 e-3	524 e-3	539 e-3
3	0	431.8	-93.4	4.80	0	-70	14	66.0 e-3	12.5 e-3	86.0 e-3
4	90	-20.3	433.1	0.82	0	0	-19	1.80 e-3	1.80 e-3	1.30 e-3
5	-90	0	0	0.35	0	0	0	300 e-6	300 e-6	400 e-6
6	90	0	0	0.09	0	0	32	150 e-6	150 e-6	40 e-6

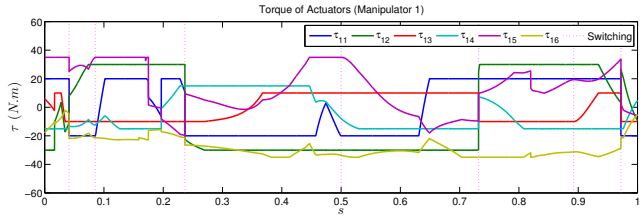

(a) Manipulator 1

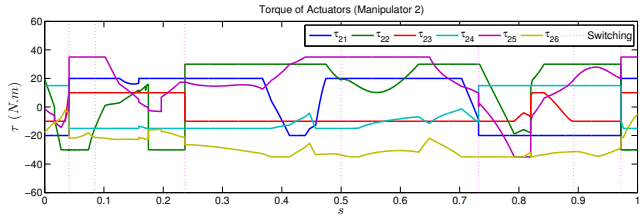

(b) Manipulator 2

Fig. 10. Actuator torques calculated for indirect procedure (example III).

VI. EFFICIENCY EVALUATION

In this section, the efficiency of the proposed algorithm is compared with one of the most recent method. We implemented the presented method in [19] for all three numerical examples solved in section V. Both methods are executed on Matlab/Simulink 9.0 enabling parallel computing on a PC (Intel i7-5930 CPU and 24 GB Memory). The forward and backward integrations performed with 1 ms as step time. The MVC is also constructed considering 1000 points through out the path. The computation time for calculating two major parts of time-optimal path, i.e. MVC and solution curve, are given in Table III for two methods as well as total computation time. The results shows that the computation time are reduced 62.2%, 74.9% and 56.8% for examples I, II and III respectively. The most reduction occurs in example II which does not need the construction of the MVC. The time consumed to calculate the MVC for examples I and III is also reduced which is due to skip of the whole construction of MVC by implementing our algorithm. Using the SPA algorithm, the computation time for calculating solution curve is substantially reduced by looking for saturated actuators in only a limited number of points, instead of determining the saturated actuators in each point which is performed in [19]. For example III, the equations of motion become more complicated which results a large computation cost to find time-optimal path. By implementing the proposed method, the computation time for applying the method presented in [19], which is 2304.3 sec, is drastically reduced to 996.2 sec. This example clearly shows the efficiency of our algorithm by saving 1308.1 sec.

VII. CONCLUSION

The problem of finding the time-optimal trajectory of a non-redundant parallel manipulator moving on a specified path is studied in this paper. Focus of this study is on the subject of reducing computational cost of the solutions obtained based on phase plane analysis. Two important issues which are sources of large computational costs were considered and resolved. The first is how to compute minimum/maximum acceleration along the path. Using the presented method, instead of determining the saturated actuators in each point which is computationally expensive, we can look for saturated actuators in only a limited number of points. The second problem is calculation of the switching points which is the most difficult part of the time-optimal solution. This paper gives a comprehensive study on this subject and all different possible situations are explored. Several examples are provided, first, to show different possibilities which may be encountered, and then to show how they are solved by means of the proposed method.

REFERENCES

[1] J. Bobrow, S. Dubowsky, and J. Gibson, "Time-Optimal Control of Robotic Manipulators Along Specified Paths," *The International Journal of Robotics Research*, vol. 4, no. 3, pp. 3–17, sep 1985.

[2] Q.-C. Pham, "A General, Fast, and Robust Implementation of the Time-Optimal Path Parameterization Algorithm," *IEEE Transactions on Robotics*, vol. 30, no. 6, pp. 1533–1540, dec 2014.

[3] F. Pfeiffer and R. Johanni, "A concept for manipulator trajectory planning," pp. 115–123, 1987.

[4] L. Zlajpah, "On time optimal path control of manipulators with bounded joint velocities and torques," in *Proceedings of IEEE International Conference on Robotics and Automation*, vol. 2. IEEE, 1996, pp. 1572–1577.

[5] T. Kunz and M. Stilman, "Time-Optimal Trajectory Generation for Path Following with Bounded Acceleration and Velocity," in *Robotics: Science and Systems VIII*. Kunz2012: Robotics: Science and Systems Foundation, jul 2012.

[6] H. Nguyen and Q.-C. Pham, "Time-Optimal Path Parameterization of Rigid-Body Motions: Applications to Spacecraft Reorientation," *Journal of Guidance, Control, and Dynamics*, vol. 39, no. 7, pp. 1667–1671, jul 2016.

[7] P. Shen, X. Zhang, and Y. Fang, "Essential Properties of Numerical Integration for Time-Optimal Path-Constrained Trajectory Planning," *IEEE Robotics and Automation Letters*, vol. 2, no. 2, pp. 888–895, apr 2017.

TABLE III
EVALUATING THE EFFICIENCY OF PROPOSED TIME-OPTIMAL ALGORITHM BY COMPARISON WITH REFERENCE [19]

Index		Computation Time (sec)					
Example		I		II		III	
Method		Ref [19]	Proposed	Ref [19]	Proposed	Ref [19]	Proposed
Time-optimal Path	MVC	5.4	1.2	5.5	—	696.3	594.0
	Solution Curve	12.6	5.6	27.9	8.4	1608.0	402.2
	Total	18	6.8	33.4	8.4	2304.3	996.2
Reduction of Computation Time (%)		62.2		74.9		56.8	

[8] S. Behzadipour and A. Khajepour, "Time-optimal trajectory planning in cable-based manipulators," *IEEE Transactions on Robotics*, vol. 22, no. 3, pp. 559–563, 2006.

[9] S. Moon and S. Ahmad, "Time optimal trajectories for cooperative multi-robot systems," in *29th IEEE Conference on Decision and Control*. IEEE, 1990, pp. 1126–1127 vol.2.

[10] J. Bobrow, J. McCarthy, and V. Chu, "Minimum-time trajectories for two robots holding the same workpiece," in *29th IEEE Conference on Decision and Control*, IEEE. IEEE, 1990, pp. 3102–3107 vol.6.

[11] S. Moon and S. Ahmad, "Time scaling of cooperative multirobot trajectories," *IEEE Transactions on Systems, Man, and Cybernetics*, vol. 21, no. 4, pp. 900–908, 1991.

[12] ——, "Time-optimal trajectories for cooperative multi-manipulator systems," *IEEE Transactions on Systems, Man and Cybernetics, Part B (Cybernetics)*, vol. 27, no. 2, pp. 343–353, apr 1997.

[13] J. McCarthy and J. Bobrow, "The number of saturated actuators and constraint forces during time-optimal movement of a general robotic system," *IEEE Transactions on Robotics and Automation*, vol. 8, no. 3, pp. 407–409, jun 1992.

[14] M. H. Ghasemi and M. J. Sadigh, "A Direct Algorithm to Compute the Switching Curve for Time-Optimal Motion of Cooperative Multi-Manipulators," *Advanced Robotics*, vol. 22, pp. 493–506, 2008.

[15] M. J. Sadigh and S. Mansouri, "Application of phase-plane method in generating minimum time solution for stable walking of biped robot with specified pattern of motion," *Robotica*, vol. 31, no. 06, pp. 837–851, feb 2013.

[16] Q.-C. Pham and Y. Nakamura, "Time-optimal Path Parameterization for critically dynamic motions of humanoid robots," in *2012 12th IEEE-RAS International Conference on Humanoid Robots (Humanoids 2012)*. IEEE, nov 2012, pp. 165–170.

[17] D. Verscheure, B. Demeulenaere, J. Swevers, J. De Schutter, and M. Diehl, "Time-optimal path tracking for robots: A convex optimization approach," *IEEE Transactions on Automatic Control*, vol. 54, no. 10, pp. 2318–2327, 2009.

[18] K. Hauser, "Fast interpolation and time-optimization with contact," *The International Journal of Robotics Research*, vol. 33, no. 9, pp. 1231–1250, aug 2014.

[19] Q.-C. Pham and O. Stasse, "Time-Optimal Path Parameterization for Redundantly Actuated Robots: A Numerical Integration Approach," *IEEE/ASME Transactions on Mechatronics*, vol. 20, no. 6, pp. 3257–3263, dec 2015.

[20] Z. Shiller and H.-H. Lu, "Computation of Path Constrained Time Optimal Motions With Dynamic Singularities," *Journal of Dynamic Systems, Measurement, and Control*, vol. 114, no. 1, p. 34, 1992.

[21] P. Corke and B. Armstrong-Helouvry, "A search for consensus among model parameters reported for the PUMA 560 robot," in *Proceedings of the 1994 IEEE International Conference on Robotics and Automation*. IEEE Comput. Soc. Press, 1994, pp. 1608–1613.

Saeed Mansouri received his B.S. and M.S. degrees in Mechanical Engineering both from Isfahan University of Technology (IUT), Isfahan, Iran in 2009 and 2011 respectively. He is currently a senior Ph.D candidate in Robotic Surgery Lab at School of Mechanical Engineering, Sharif University of Technology, Tehran, Iran. His research interests include humanoid robots, medical robotics, optimal control and mechatronics.

Mohammad Jafar Sadigh received his B.S. and M.S. degrees in Mechanical Engineering both from Isfahan University of Technology (IUT), Isfahan, Iran in 1986 and 1989, respectively, and PhD from McGill University, Montreal, Canada in 1995. Between 1995 and 2014, he was with the Department of Mechanical Engineering at Isfahan University of Technology (IUT) and is currently Assistant Professor at University of Tehran (UT). His research interests are system dynamics, robotics, humanoid robots and rehabilitation. Also, he is very active in the field of science park development and technology management and now is the head of University of Tehran Science and Technology Park.

Masoud Fazeli received his bachelors and masters degrees at Mechanical Engineering from Isfahan University of Technology (IUT), Isfahan, Iran in 2009 and 2011 respectively. His research has focused on humanoid robots, underwater systems, hybrid force control and simulation in robotics.